Micro- and Macrothermal Analysis of a Bioactive Surface-Engineered Polymer Formed by Physical Entrapment of Poly(ethylene glycol) into Poly(lactic acid)

Jianxin Zhang,[†] Clive J. Roberts,*[,†] K. M. Shakesheff,[‡] Martyn C. Davies,[†] and Saul J. B. Tendler[†]

Laboratory of Biophysics and Surface Analysis, School of Pharmaceutical Sciences, University of Nottingham, Nottingham NG7 2RD, UK, and Tissue Engineering Group, School of Pharmaceutical Sciences, University of Nottingham, Nottingham NG7 2RD, UK

Received August 19, 2002; Revised Manuscript Received December 13, 2002

ABSTRACT: Poly(DL-lactic acid) (PLA) materials have been surface engineered via an entrapment method to present high densities of poly(ethylene glycol) (PEG) to control protein adsorption. The resultant change in physical properties was characterized on the surface and bulk of the entrapped PEG/PLA system through microthermal analysis by scanning thermal microscopy (SThM). It was found that the inclusion of the PEG significantly reduced the glass transition temperature (T_g) of the modified PLA and that the magnitude of this T_g reduction remained unchanged throughout the PEG-modified PLA regions. This suggests that the entrapped PEG was in a miscible state with, and homogeneously distributed into, the PLA. This finding was confirmed using macrothermal analysis by differential scanning calorimetry. The amount of the PEG entrapped in the modified region was calculated to be 18 wt %. In addition, a sharp contrast was observed in the SThM thermal conductivity data on cross-sectioned samples designed to reveal the boundary between the modified and unmodified regions of the PLA. This unambiguously demonstrates that the physical properties of the PLA surface and near surface have been modified by the entrapment of PEG. We propose that the observed thermal contrast results from the temperature dependency of thermal conductivity (λ) of the parent PLA being altered by the inclusion of miscible PEG.

Introduction

Poly(DL-lactic acid) (PLA) is extensively used in biomaterial applications such as resorbable sutures, scaffolds, and drug delivery devices.[1−19] Recent developments in tissue engineering and drug delivery have required the immobilization of biologically active molecules on the surfaces of PLA-based devices[1] to promote or introduce favorable biointeractions within biological environments.[2,3] As part of achieving such a goal, the introduction of a biocompatible polymer, poly(ethylene glycol) (PEG), onto the surface has been employed for rendering PLA resistant to cell or protein adsorption,[4−6] thus reducing complications such as biofouling and thrombus formation on contact with biological fluids.[7−9]

In the past years, various chemical[10,12−14] and physical[11,15−17] methods have been developed for modifying the surface of biomaterials. Recently, we have developed a new strategy for engineering PEG and poly(L-lysine) (PLL) into PLA,[15] which is based on a method devised by Hubbell for the modification of poly(ethylene terephthalate) (PET).[16,17] The advantages of our strategy include the following: First, it can readily entrap high densities of the modifying materials. Second, it is simple and does not need the synthesis of new polymer structures or alter the advantageous mechanical properties of the bulk PLA.[18]

The incorporation of PEG into PLA facilitates control of protein adsorption and minimizes nonspecific cell adhesion.[19] In this study, we focus on the investigation of the physical properties of both the PLA surface and bulk after the PEG inclusion. This was carried out by using localized thermal analysis (LTA) mode of scanning thermal microscopy (SThM) and differential scanning calorimetry (DSC). Here we refer to LTA as microthermal analysis[20] and DSC as macrothermal analysis, based upon their respective sampling volumes.

SThM is characterized by its combination of the imaging capability of an atomic force microscope (AFM) with spatially resolved LTA.[20] The difference between AFM and SThM is that a conventional AFM probe is replaced with a resistive Wollaston wire. This resistive wire simultaneously acts as both a highly localized heating source and a temperature sensor.[20−22] As a heater, it supplies energy to raise the local temperature of a sample surface to a required level, while as a sensor it monitors the sample temperature. Accordingly, it can provide not only topographic features as a normal AFM does (albeit at a lower resolution) but also thermal energy related contrast that is specifically associated with the thermal conductivities. The spatial resolution of imaging is currently limited to about 1 μm with the V-shaped Wollaston probe due to its large size (75 μm diameter silver wire containing a 5 μm diameter platinum/10% rhodium core[20]). When SThM is operated in the imaging mode, a constant temperature is kept at the tip. The energy required to maintain at such a constant level is then recorded to build up a thermal contrast image. LTA is used to determine transition temperatures at an individual point of a sample surface by placing the probe onto the surface and ramping the temperature at a linear scan rate. The transition temperature value is often taken as the temperature at which the probe deflection or power signal changes suddenly.[21,23] Since its commercial launch in 1998, SThM has found an increasing number of applications

[†] Laboratory of Biophysics and Surface Analysis.
[‡] Tissue Engineering Group.
* Corresponding author: e-mail Clive.Roberts@nottingham.ac.uk.

10.1021/ma0213551 CCC: $25.00
Published on Web 01/23/2003

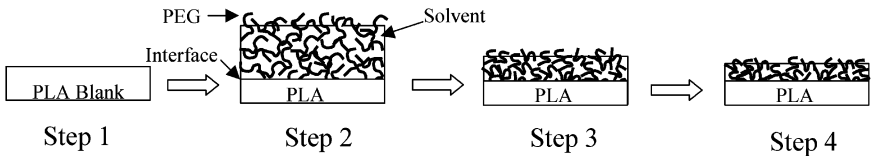

Figure 1. Schematic of the sample preparation processes: Step 1 is the formation of a PLA blank disk. Step 2 involves swelling the PLA disk and diffusing PEG molecules into the disk substrate in a PEG/TFE/water solution. In step 3, the PEG molecules are entrapped inside the PLA by deswelling the swollen disk by addition of a large excess of water into the solution. Step 4 is the removal of the possible residual TFE and water from the substrate by drying.

due to its ability to correlate thermal and topographic data.[20−32]

Relevant to the current entrapped PEG/PLA system, there exist several studies[33−35] on the phase behaviors of the PEG/PLA polymer blends in the literature. Miscible PEG/PLA blends have been prepared by melt processing,[33] a solvent casting technique,[34] and precipitation method.[35] However, high PEG loadings (above 50 wt %) in the PEG/PLA blends resulted in a macrophase separation driven by crystallization of the PEG.[33] By using a solution processing technique similar to the current approach, Desai and Hubbell[16,17] have also demonstrated that a phase-mixed structure can be created in a thermodynamically immiscible PEG/PET polymer system, since the homogeneously dispersed PEG was frozen in the swollen PET by a rapid nonsolvent quench process.

Experimental Section

Sample Preparation and Procedures of Entrapping PEG into PLA. Poly(DL-lactic acid) transparent pellets (Alkermes, $M_w = 85\,000$) were first formed into small sample disks (ca. 1.5 cm in diameter and 0.3 mm thick). This was carried out by softening the pellets sandwiched between two clean glass slides on a hot plate. The plate temperature was preset at 150 °C. The PLA disks were then allowed to cool to room temperature in air prior to removal from the glass slides. As schematically shown in Figure 1, the surface entrapment was carried out by immersing the PLA disks into a 1 mL modifying solution of 10% w/v PEG (Polysciences Inc., $M_w = 18\,500$) in a mixture of a 2,2,2-trifluoroethanol (TFE, 10% v/v) and double distilled water (90% v/v) for 24 h. This solution partially solvates and expands the PLA to facilitate the inclusion of the PEG. A large excess of distilled water was then added into the modifying solution. The modified PLA disks were subsequently removed and washed in distilled water for 30 min. They were finally dried in a desiccator at room temperature for a week to remove the possible residual TFE and water. These dried samples were subjected to microthermal and macrothermal analysis.

Instrumentation. Microthermal analysis was performed by a 2990 microthermal analyzer (m-TA) (TA Instruments, New Castle, DE) equipped with a V-shaped Wollaston thermal probe at room temperature of 18−20 °C. Prior to experiments, the thermal probe was calibrated at 10 °C/s under an applied force signal equating to 10 nA with three semicrystalline polymers of PEG, polypropylene (PP), and nylon-6. The melting temperatures (T_m) of the calibration materials were predetermined to be 62 °C (PEG), 158 °C (PP), and 217 °C (nylon-6) on a Perkin-Elmer DSC-7 at 10 °C/min which had been calibrated using an indium standard. Topography and thermal conductivity images were simultaneously acquired on the surface of the modified PLA samples at 50 μm/s with the probe held at 45 °C. LTA experiments were all performed at 10 °C/s, unless specified otherwise. Similar experiments were also conducted on the microtomed (RMC MT7 cryoultramicrotome) surface of the entrapped PLA samples. It was estimated that the penetration depth of heat into a sample surface in LTA measurements is of the order of a few micrometers based on a sampling volume a few cubic micrometers.[24] Data analysis was conducted with the Universal Analysis program supplied with the analyzer. A Perkin-Elmer DSC-7 was used to measure the transition temperatures of pure PEG, pure PLA, and the modified PLA. In DSC analysis, a sample mass used was about 10 mg. It was estimated that the PEG penetration depth was 35 μm. Therefore, the total thickness of the PEG-modified layer for DSC samples was approximately 70 μm.

Results and Discussion

Microthermal Analysis of the PEG/PLA Surface. Previously, we have demonstrated by high-resolution X-ray photoelectron spectroscopy (XPS) that high densities of poly(ethylene glycol) are incorporated into PLA sample surfaces by the physical entrapment method.[15] This means that the chemistry and properties of the PEG-modified PLA have been altered. However, thermal conductivity images (not shown) obtained by SThM provide little contrast on the PEG-modified PLA surface. This may suggest a homogeneous thermal constitution at the surface. To ascertain whether this has occurred and to examine whether the PEG inclusion has brought about a detectable change in the physical properties of the PLA, LTA was performed on the sample disk surface. It has been known that LTA analysis can be used to identify the constituents of multicomponent systems.[24] Pure PLA and PEG were first examined as references.

Figure 2 shows LTA data recorded for PLA alone (Figure 2a), PEG alone (Figure 2b), and the PEG-entrapped PLA system (Figure 2c). This figure displays the sensor, power signals of the probe, and the corresponding differential of the power with respect to temperature. The sensor signal measures the vertical deflection of the probe as the probe temperature is raised.[21] The transition temperature is defined here as the temperature where the probe deflection abruptly drops. It appears that there is no obvious change in the power signals (straight lines) of the pure PLA and PEG (Figure 2a,b). However, a clear difference in the derivative power signals can be seen between the amorphous PLA and semicrystalline PEG, which also happened to other polymers.[23] The PLA is characterized by a small step at its T_g whereas the PEG by a relatively large downward peak at its T_m. These two different features are similar in shape to the DSC curves of the respective amorphous and crystalline polymers and thus are attributable to a heat capacity variation at T_g and enthalpy change at T_m. Therefore, these characteristics can be used to identify the morphological state of a polymer.

Figure 2c is a representative LTA trace obtained from many different locations of the PEG-modified PLA disk surface. It was noted that such traces were highly repeatable with the average transition temperature determined being 54 °C within a variation of about 1−3 °C. Such a small variation was also observed in measuring the T_g and T_m of the PLA and PEG homogeneous linear polymers (data not shown) and has been reported

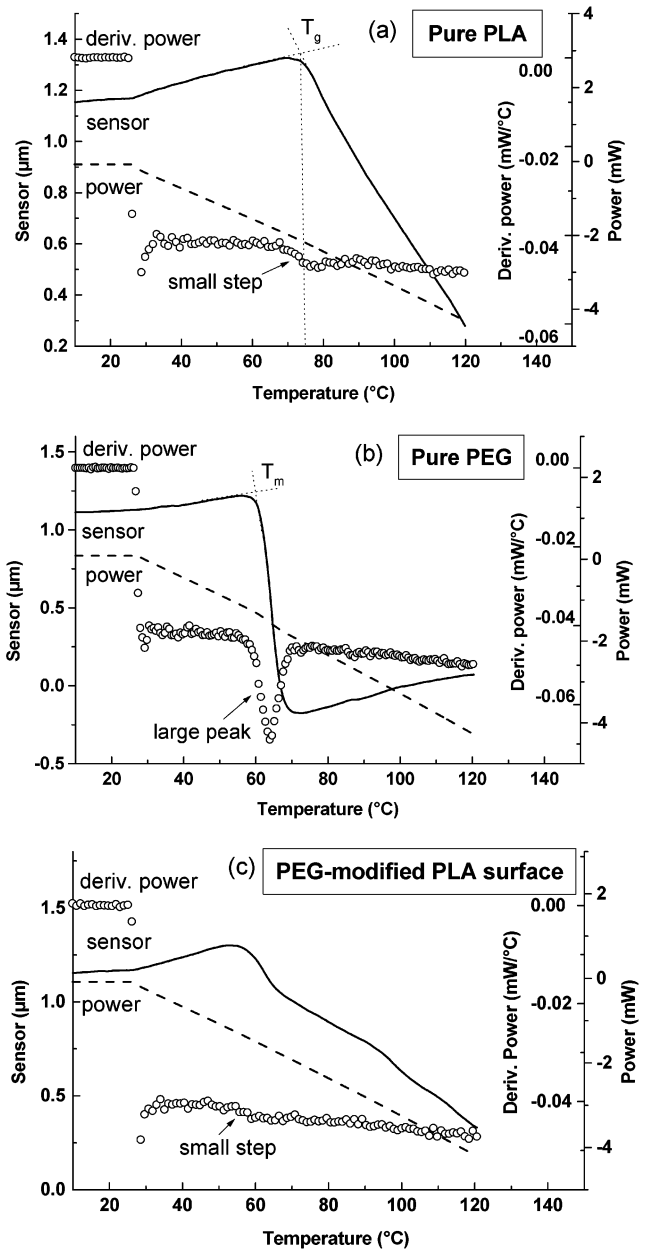

Figure 2. Representative LTA traces recorded from the top surfaces of the pure PLA (a), pure PEG (b), and PEG-modified PLA (c). (a) and (b) show that the T_g of the pure amorphous PLA is characterized by a small step change in its derivative power signal, while the T_m of the PEG crystallines by a large downward peak. (c) indicates that the modified PLA is in an amorphous state as judged by the presence of a small step in its derivative power; the T_g of the PLA is dramatically reduced from 74 to 54 °C after the PEG inclusion.

previously.[31] However, this consistency has been absent on highly cross-linked thermoset polymers due to the heterogeneous distribution of the cross-link density in these materials.[32] Therefore, such a small variation confirms that the entrapped PEG was homogeneously distributed in the PLA surface, consistent with the thermal conductivity data. It also demonstrates the reproducibility of the transition temperature measurements in LTA.

The average T_g for the PLA was 74 °C and the average T_m for the PEG was 59 °C. In comparison to the pure PLA, the transition temperature of the PEG/PLA system was significantly reduced from 74 to 54 °C, suggesting that the physical properties of PLA have indeed been modified by the PEG. Moreover, a small slope in the derivative power of the PEG/PLA (Figure 2c) indicates that the transition at 54 °C is a glass transition, and hence the PEG entrapped PLA is in an amorphous state. On the basis of the observed homogeneity and the large reduction in the T_g, we propose that the entrapped PEG is in a miscible state with PLA. The PEG in fact acts as a plasticizer inside PLA and thus reduces the PLA T_g effectively due to its very low transition temperature ($T_g \sim -75$ to -65 °C[33]). This is possible, considering that the presence of the diluent PLA frustrates the PEG crystallization. As a result, a crystallization-induced phase separation is suppressed which is a driving force for producing PEG- and PLA-rich domains in PLA/PEG polymer blends.[34] We have examined the PEG-engineered PLA surface under an atomic force microscope (Nanoscope IIIa Dimension 3000 AFM, Digital Instrument) following a method described in ref 44. The results showed no evidence of crystallization (data not shown).

Microthermal Analysis of the PEG/PLA Cross-Sectioned Surface. We have shown that the physical properties of the PEG/PLA top surface were significantly modified. It is also important to know whether the modification had extended into the bulk of the PLA disk. To do this, the sample disks were carefully microtomed. Imaging acquisition was carried out on this cross-sectioned surface. Figure 3a shows the topographic image and the histogram of the topography, while Figure 3b shows the corresponding thermal conductivity image and the data histogram. It is apparent that little information can be deduced from Figure 3a. However, a strong contrast can be clearly seen in the thermal conductivity images—the lighter contrast with the data indicating higher thermal conductivity resulted from the "shell" of the PEG/PLA disk, whereas the darker regions (lower thermal conductivity) from the "core". Clearly this distinctive contrast is independent of the topography and therefore was generated by the change in the properties of the PLA. This change is further supported by the two distinguished peak distributions in the histogram of thermal conductivity data. The origin of the observed contrast formation will be discussed later. It is very evident that the PEG had diffused into the near-surface bulk region of the PLA, in this case about 35 μm in the conditions employed. The implication for this is that if the outer surface is eroded within a biological environment, the newly exposed surface can still maintain its protein-repelling function. The penetration depth of the PEG modification can be controlled as required by manipulating the sample preparation parameters such as the PEG concentration in the solution, the cosolvent mixing ratio, and impregnation time.[15]

The SThM probe was then positioned onto the two distinct regions evident in Figure 3b to determine the localized transition temperatures. Representative sensor signals obtained are presented in Figure 4a. The corresponding power and derivative power signals shown in Figure 4b demonstrate that both of the core and shell are in an amorphous state. It was determined from many points (such as points A−H shown in Figure 3b) that the T_g's of the core and shell are approximately 74 and 53 °C, respectively, with an error of about 1−3 °C. The T_g of the core is nearly identical to that of the pure PLA and therefore suggests that the core remained unchanged during the diffusion and entrapment pro-

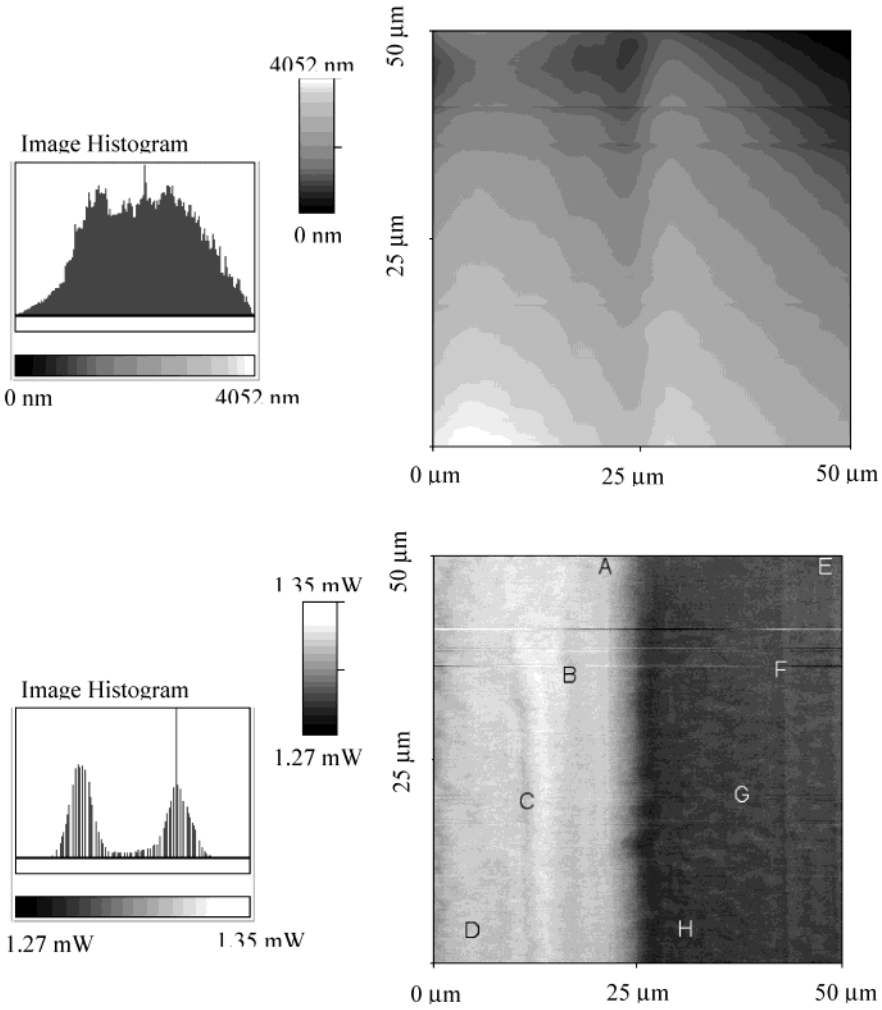

Figure 3. Topographic image (a, upper) and thermal conductivity image (b, lower) acquired on the microtomed surface of the PEG-modified PLA; the sharp contrast boundary in (b) indicates that the physical properties of the PLA disk shell are modified by the PEG entrapped.

cesses. The small variation of the T_g values across the shell region indicates that the shell was uniformly modified throughout. The large difference (21 °C) in T_g between the shell and core supports our conclusion of the entrapped PEG being miscible with the PLA.

The observed homogeneity of the shell and the shell–core sharp interface suggest that the PEG diffusion represents a case II process, whereby the diffusion process is characterized by a sharp penetrant front which advances into the polymer linearly with time and a uniform penetrant concentration behind the front.[36] In the current case, it is possible that the swelling or formation of the PLA gels governs the rate of the PEG diffusion. Once the PLA gels form, the PEG molecules in the solution will quickly fill in the "loose" and disentangled PLA molecular chains and reach equilibrium. When the gel is collapsed by a less favorable solvent (water), the uniformly dispersed PEG will be entrapped or "frozen"[16,17] in the shrunken gel. If the composition fluctuation had occurred to the shell, a large difference in T_g should have been observed at least on the modified disk surface and locations near the shell/core interface (see Figure 3b).

To our knowledge, there are no thermal conductivity (λ) data for the PLA or PEG/PLA system available in the open literature. To explain the origin for the formation of the thermal contrast in Figure 3b, we therefore propose in Figure 5 the relationship between λ and temperature (T) for the core and shell regions. This $\lambda-T$ relationship is produced on the basis of a general curve for amorphous polymers summarized by Van Krevelen.[37] It can be seen from Figure 5 that λ increases initially when T is below T_g, reaches a maximum at T_g, and then decreases above T_g with a reduced slope. Such a temperature dependence of λ is generally governed by variations in the mean free path (L) of phonons which are considered to be main heat carriers.[38] As addressed previously, the PEG inside the PLA functions as a plasticizer and thus reduces interchain interactions and promotes the mobility of chain segments. As a result, the overall effect of the addition of PEG is to decrease L and increase λ of the PLA below T_g (see Figure 5). Above T_g, however, the reverse is true due to an opposing effect on L. Therefore, when the SThM probe scans at a constant temperature below the shell T_g, a thermal contrast is generated between the shell and core as evidenced in Figure 3b. This proposal is also consistent with the experimental results of the thermal conductivities of pure poly(vinyl chloride) (PVC) and plasticized PVC[38,39] below and above their T_g's.

Macrothermal Analysis of the PEG/PLA Bulk. Since SThM is a relatively new technique, improvements in the technique and its applications in different areas are being continuously explored. Therefore, appropriate interpretation of the results obtained from this technique sometimes still needs to be considered and

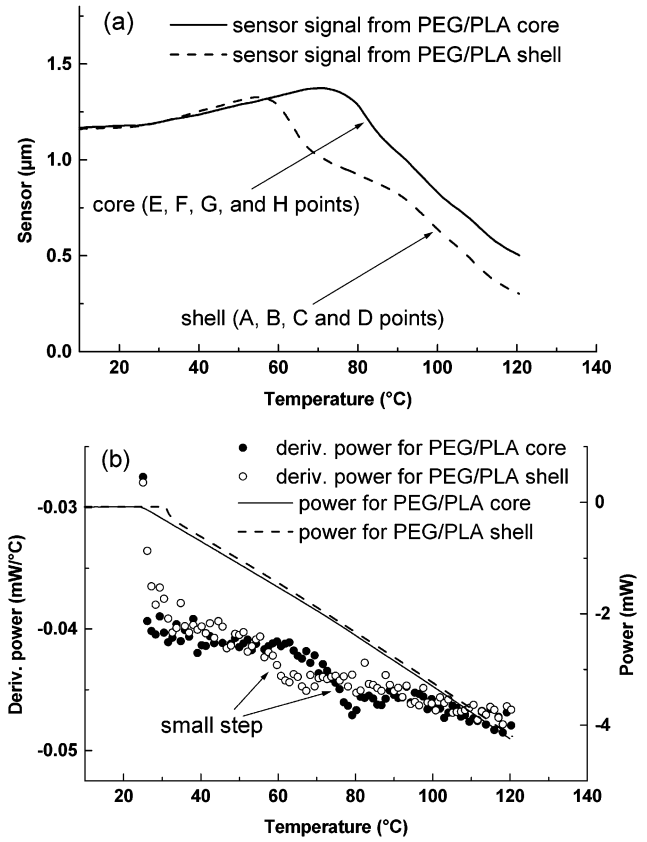

Figure 4. Representative LTA data obtained from the core and shell of the PEG-modified PLA sample disk. (a) The sensor signals, showing that the T_g of the core remains unchanged as that of the pure PLA, whereas the T_g of the shell is significantly decreased by about 20 °C. (b) The power and derivative power signals, showing that both the core and shell are amorphous.

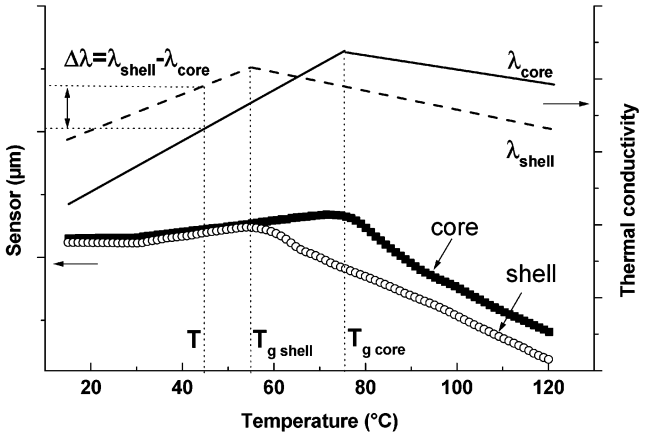

Figure 5. Actual data and schematic relationship between the thermal conductivity and temperature for the shell and core of the PEG-modified PLA sample disk.

confirmed with other more conventional techniques. In this study, DSC was used for this purpose. The PLA T_g was determined to be 47 °C (Figure 6a), and the PEG T_m was 62 °C (Figure 6b). It should be noted in Figure 6a that an "overshoot" in the DSC trace was caused by enthalpy relaxation or recovery.[40] Its occurrence is dependent upon the thermal history of a polymer. Figure 6c demonstrates that there are two T_g's for the PEG/PLA, characterized by two heat capacity jumps. With the help of the SThM spatial information (Figure 3b), it is reasonable to believe that the higher T_g at 47 °C is attributed to the core of the PEG/PLA and the lower T_g at 16 °C to the shell. From these DSC results, similar conclusions can be made as follows: First, the core has not been modified. The nonmodification is also evidenced by the appearance of the enthalpy relaxation overshoot on the PEG/PLA DSC curve which indicates that the thermal history of the core remained intact. Second, the bulk sample disk is amorphous since there was no T_m endothermic peak. Third, as with the microthermal analysis, a significant difference (31 °C) in T_g was found between the core and shell. This again signifies the miscibility of the PEG and PLA because a miscible polymer blend always produces a T_g intermediately located between the T_g's of its constituents.

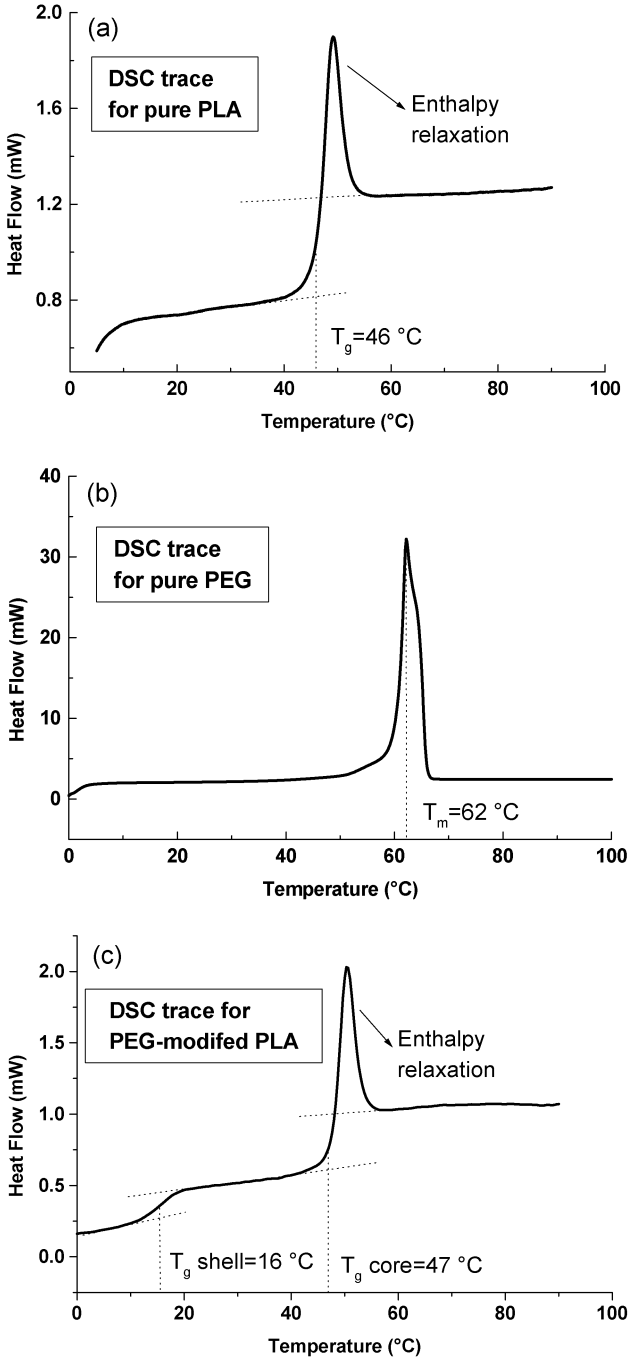

Figure 6. DSC traces for the pure PLA (a), pure PEG (b), and PEG-modified PLA (c). (c) demonstrates that there are two T_g's in the PEG-modified PLA. The lower T_g (16 °C) is attributed to the shell and the higher T_g (47 °C) to the core.

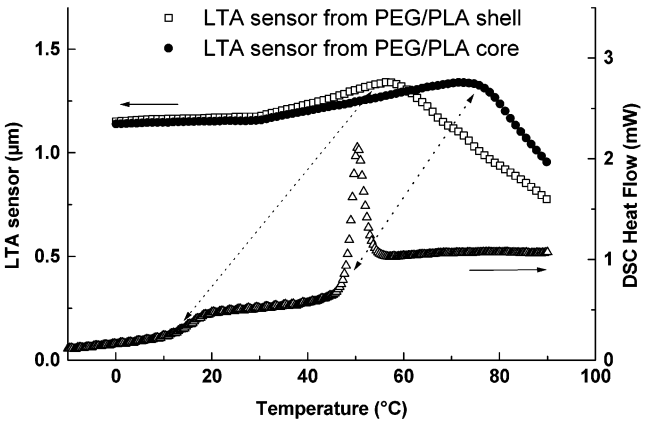

Figure 7. Comparison of the difference in the T_g values determined from LTA and DSC for the PEG-modified PLA.

We also used the T_g's determined from DSC to estimate the amount of the PEG inclusion following the Fox equation

$$\frac{1}{T_g} = \frac{w_1}{T_{g1}} + \frac{w_2}{T_{g2}} \tag{1}$$

or alternatively

$$w_1 = \frac{T_{g1}(T_{g2} - T_g)}{T_g(T_{g2} - T_{g1})} \tag{2}$$

where T_g is the glass transition temperature (16 °C) of the PEG/PLA system, T_{g1} and T_{g2} (47 °C) are the glass transition temperatures of PEG and PLA, respectively, and w_1 and w_2 are the weight fractions of the PEG and PLA, respectively. Since the glass transition temperature of PEG (−75 to −65 °C[33]) is difficult to obtain experimentally, we take its value as −70 °C. According to eq 2, the amount of the PEG incorporated into the shell is calculated to be 18 wt %, which is in good agreement with our previously determined values by XPS.[15]

It is evident that the DSC data strongly support our conclusions made from the microthermal analysis. However, the T_g's obtained from LTA were significantly higher than those from DSC, as demonstrated in Figure 7 by comparison. We have found that this phenomenon consistently occurred with other polymers (results not shown) and have been attributed it partly to the heating rate (q) effect on the polymer T_g. Figure 8 demonstrates this effect on the pure PLA T_g by varying systematically the q range 0.1−25 °C/s (equivalent to 6−1500 °C/min). It shows that the relationship between the T_g and q can be described by eq 3.

$$T_g = 50.2 + 8.6 \log(q) \tag{3}$$

Briefly, the other possible reasons are that the sample surface temperature in fact lags behind the probe temperature due to the contact thermal resistance existed in the probe−sample interface.[41−43] In addition, there is a temperature gradient extending away from the heated tip down into a sample surface, and its value will be affected by the properties of the sample and heating rate.[45] Our results also demonstrate that the PEG T_m was less affected (Figure 2b), which is consistent with an earlier observation on melting phenomena.[28] Therefore, the T_g data obtained from LTA can only be treated as qualitative rather than quantitative.

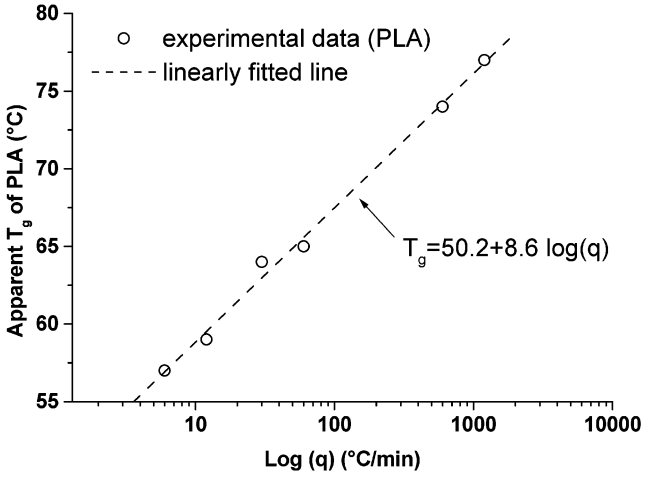

Figure 8. Apparent T_g of pure PLA measured from LTA as a function of q.

However, the qualitative nature of the LTA T_g data does not affect our conclusions in this study.

Conclusions

Poly(DL-lactic acid) (PLA) materials have been surface engineered to present high densities of poly(ethylene glycol) (PEG) designed to control protein adsorption via an entrapment method strategy we have previously reported.[15] The change in the physical properties of the PLA resulting from the PEG modification has been subsequently studied with a microthermal analysis technique of scanning thermal microscopy (SThM). It has been found that the glass transition temperature (T_g) of the PEG-modified PLA is significantly reduced, and the thermal conductivity is increased below its T_g. The SThM results also demonstrate that the magnitude of the T_g reduction is the same throughout the PEG-modified PLA regions. This suggests that the PEG molecules are homogeneously entrapped inside and in a miscible state with the PLA. Thus, the PLA T_g has been effectively depressed. However, the properties of the PLA sample disk "core" remain intact during the entrapment process since its T_g is the same as that of the untreated PLA materials. The homogeneous properties of the modified and unmodified regions imply that the PEG diffusion is a case II process. This is also evidenced by a distinctive contrast in the SThM thermal conductivity (λ) image formed between these two areas. The results as measured with differential scanning calorimetry (DSC) fully support the above conclusions and explanations. The amount of the PEG entrapped is calculated to be about 18 wt %. Finally, we propose that the formation of the observed SThM thermal contrast originates from the miscible PEG inclusion altering the temperature dependency of the PLA λ. This leads to the engineered PLA having higher λ values below T_g and lower λ values above T_g as compared to the parent PLA.

Acknowledgment. We thank the EPSRC Multi-User Equipment Initiative for funding the SThM instrument and J.Z. postdoctoral fellowship. We also thank Molecular Profiles Ltd. for access to cryogenic ultramicrotome facilities.

References and Notes

(1) Langer, R. *Ann. Biomed. Eng.* **1995**, *23*, 101.
(2) Hubbell, J. A. *Curr. Opin. Biotechnol.* **1999**, *10*, 123.

(3) Ratner, B. D. *Biosens. Bioelectron.* **1995**, *10*, 797.
(4) Ikada, Y. *Biomaterials* **1994**, *15*, 725.
(5) Griffith, L. G. *Acta Mater.* **2000**, *48*, 263.
(6) Elbert, D. L.; Hubbell, J. A. *Annu. Rev. Mater. Sci.* **1996**, *26*, 365.
(7) Suggs, L. J.; West, J. L.; Mikos, A. G. *Biomaterials* **1999**, *20*, 683.
(8) Elbert, D. L.; Hubbell, J. A. *Chem. Biol.* **1998**, *5*, 177.
(9) Deible, C. R.; Petrosko, P.; Johnson, P. C.; Beckman, E. J.; Russell, A. J.; Wagner, W. R. *Biomaterials* **1998**, *19*, 1885.
(10) Gombotz, W. R.; Guanghui, W.; Horbett, T. A.; Hoffman, A. S. *J. Biomed. Mater. Res.* **1991**, *25*, 1547.
(11) Dunn, S.; Coombes, A. G. A.; Garnett, M. C.; Davis, S. S.; Davies, M. C.; Illum, L. *J. Controlled Release* **1997**, *44*, 65.
(12) Bearinger, J. P.; Castner, D. G.; Healy, K. E. *J. Biomater. Sci., Polym. Ed.* **1998**, *9*, 629.
(13) Han, D. K.; Hubbell, J. A. *Macromolecules* **1997**, *30*, 6077.
(14) Huh, K. M.; Bae, Y. H. *Polymer* **1999**, *40*, 6147.
(15) Quirk, R. A.; Davies, M. C.; Tendler, S. J. B.; Shakesheff, K. M. *Macromolecules* **2000**, *33*, 258.
(16) Desai, N. P.; Hubbell, J. A. *Macromolecules* **1992**, *25*, 226.
(17) Desai, N. P.; Hubbell, J. A. *Biomaterials* **1991**, *12*, 144.
(18) Drumright, R. E.; Gruber, P. R.; Henton, D. E. *Adv. Mater.* **2000**, *12*, 1841.
(19) Lucke, A.; Tessmar, J.; Schnell, E.; Schmeer, G.; Göpferich, A. *Biomaterials* **2000**, *21*, 2361.
(20) Hammiche, A.; Reading, M.; Pollock, H. M.; Song, M.; Hourston, D. J. *Rev. Sci. Instrum.* **1996**, *67*, 4268.
(21) Hammiche, A.; Hourston, D. J.; Pollock, H. M.; Reading, M.; Song, M. *J. Vac. Sci. Technol.* **1996**, *B14*, 1486.
(22) Hammiche, A.; Bozec, L.; Conroy, M.; Pollock, H. M.; Mills, G.; Weaver, J. M. R.; Price, D. M.; Reading, M.; Hourston, D. J.; Song, M. *J. Vac. Sci. Technol.* **2000**, *B18*, 1322.
(23) Price, D. M.; Reading, M.; Hammiche, A.; Pollock, H. M. *Int. J. Pharm.* **1999**, *192*, 85.
(24) Pollock, H. M.; Hammiche, A. *J. Phys. D*: *Appl. Phys.* **2001**, *34*, R23−R54.
(25) Royall, P. G.; Kett, V. L.; Andrews, C. S.; Craig, D. Q. M. *J. Phys. Chem. B* **2001**, *105*, 7021.
(26) Fryer, D. S.; Nealey, P. F.; de Pablo, J. J. *Macromolecules* **2000**, *33*, 6439.
(27) Buzin, A. I.; Kamasa, P.; Pyda, M.; Wunderlich, B. *Thermochim. Acta* **2002**, *381*, 9.
(28) Royall, P, G.; Craig, D. Q. M.; Grandy, D. B. *Thermochim. Acta* **2001**, *380*, 165.
(29) Grandy, D. B.; Hourston, D. J.; Price, D. M.; Reading, M.; Silva, G. G.; Song, M.; Sykes, P. A. *Macromolecules* **2000**, *33*, 9348.
(30) Gorbunov, V.; Fuchigami, N.; Stone, M. Grace, M.; Tsukruk, V. V. *Biomacromolecules* **2002**, *3*, 106.
(31) Moon, I.; Androsh, R.; Chen, W.; Wunderlich, B. *J. Therm. Anal. Calorim.* **2000**, *59*, 187.
(32) Tillman, M. S.; Takatoya, T.; Hayes, B. S.; Seferis, J. C. *J. Therm. Anal. Calorim.* **2000**, *62*, 599.
(33) Sheth, M.; Kumar, R. A.; Dave, V.; Gross, R. A.; McCarthy, S. P. *J. Appl. Polym. Sci.* **1997**, *66*, 1495.
(34) Younes, H.; Daniel, C. *Eur. Polym. J.* **1988**, *24*, 765.
(35) Nijenhuis, A. J.; Colstee, E.; Grijpma, D. W.; Pennings, A. J. *Polymer* **1996**, *37*, 5849.
(36) Thomas, N. L.; Windle, A. H. *Polymer* **1982**, *23*, 529.
(37) Van Krevelen, D. W. *Properties of Polymers*; Elsevier: Amsterdam, 1972.
(38) Dashora, P.; Gupta, G. *Polymer* **1996**, *37*, 231.
(39) Eiermann, K.; Hellwege, K. H. *J. Polym. Sci.* **1962**, *57*, 99.
(40) Tant, M. R.; Wilkes, G. L. *Polym. Eng. Sci.* **1981**, *21*, 874.
(41) Shi, L.; Plyasunov, S.; Bachtold, A.; McEuen, P. L.; Majumdar, A. *Appl. Phys. Lett.* **2000**, *77*, 4295.
(42) Gomes, S.; Trannoy, N.; Grossel, P.; Depasse, F.; Bainier, C.; Charraut, D. *Int. J. Therm. Sci.* **2001**, *40*, 949.
(43) Fried, E. In *Thermal Conductivity*; Tye, R. P., Ed.; Academic Press: London, 1969; Vol. 2.
(44) Zhang, J.; Busby, A. J.; Roberts, C. J.; Chen, X.; Davies, M. C.; Tendler, S. J. B.; Howdle, S. M. *Macromolecules* **2002**, *35*, 8869.
(45) Inuoue, T.; Uehara, T. *J. Phys. IV* **1999**, *9*, 341.

MA0213551